Journal of Hazardous Materials 161 (2009) 1024–1034

Contents lists available at ScienceDirect

Journal of Hazardous Materials

journal homepage: www.elsevier.com/locate/jhazmat

Effects of iron type in Fenton reaction on mineralization and biodegradability enhancement of hazardous organic compounds

Eakalak Khan[a,*], Wanpen Wirojanagud[b,c], Nawarat Sermsai[d]

[a] Department of Civil Engineering, North Dakota State University, Fargo, ND 58105, USA
[b] Research Center for Environmental and Hazardous Substance Management, Khon Kaen University, Khon Kaen 40002, Thailand
[c] Department of Environmental Engineering, Khon Kaen University, Khon Kaen 40002, Thailand
[d] National Center of Excellence for Environmental and Hazardous Waste Management, Chulalongkorn University, Bangkok 10330, Thailand

ARTICLE INFO

Article history:
Received 27 August 2007
Received in revised form 14 April 2008
Accepted 15 April 2008
Available online 22 April 2008

Keywords:
Dissolved organic carbon
Biodegradable dissolved organic carbon
Degradation by-products
Kinetics
Fenton reaction
Iron type

ABSTRACT

The mineralization and biodegradability increase and their combination of two traditional and two relatively new organic contaminants by Fenton reagents with three different types of iron, Fe^{2+}, Fe^{3+}, and Fe^{0} were investigated. The traditional contaminants examined were trichloroethene (TCE) and 2,4-dichlorophenol (2,4-DCP) while 1,4-dioxane (1,4-D) and 1,2,3-trichloropropane (TCP) were studied for the relatively new contaminants. The mineralization and biodegradability were represented by dissolved organic carbon (DOC) reduction and the ratio of biodegradable dissolved organic carbon and DOC, respectively. For all four contaminants, Fenton reagent using Fe^{2+} was more effective in the DOC reduction than Fenton reagents using Fe^{3+} and Fe^{0} in most cases. The types of Fe that provided maximum biodegradability increase were not the same for all four compounds, Fe^{3+} for TCE, Fe^{0} for 2,4-DCP, Fe^{2+} for 1,4-D, and Fe^{3+} for TCP. When the combination of DOC elimination and biodegradability increase (least refractory fraction) was considered, Fe^{2+} was the best choice except for 2,4-DCP which was susceptible to Fe^{0} catalyzed Fenton reagent the most. The least refractory fractions remaining after 120 min of reaction were 20–25% for TCE, 2,4-DCP, and TCP and 30–40% for 1,4-D. The iron type in Fenton reaction also affected the type of mineralization kinetics of TCE, 2,4-DCP, and TCP as well as the types of degradation by-products of these contaminants. Some of the by-products found, such as isopropanol and propionic aldehyde, which were produced from Fe^{0} catalyzed Fenton degradation of TCP, have not been previously reported.

1. Introduction

Degradation of organic contaminants by Fenton reaction results in mineralization and/or biodegradability enhancement. The ratio of biochemical oxygen demand (BOD) and chemical oxygen demand (COD) has been used to represent the biodegradability of both collective and specific organic contaminants [1–6]. Mater et al. [1] observed that Fenton reaction increases the BOD at 5 days (BOD_5)/COD ratio of compounds in water contaminated with crude petroleum by 3.8 times. Lopez et al. [2] and Batarseh et al. [3] enhanced BOD_5/COD of mature landfill leachate using Fenton reagent. The BOD/COD ratio was used to indicate biodegradability changes in the photo-Fenton degradation of 4-chlorophenol [4], sulfamethoxazole [5], diuron and linuron [6].

The ratio of BOD/COD has some limitations, such as poor precision and low sensitivity for low organic concentration water samples. Khan et al. [7] applied conventional Fenton reagent to degrade low-level *p*-nitrophenol in water. The parameters used to indicate the mineralization and biodegradability were dissolved organic carbon (DOC) and the ratio of biodegradable dissolved organic carbon (BDOC) and DOC (BDOC/DOC), respectively. The BDOC analysis measures the portion of organic carbon that can be mineralized by heterotrophic bacteria [8] or the portion of DOC that is biodegradable [9]. BDOC/DOC is more sensitive and precise than BOD/COD [9]. There is no relationship between BDOC/DOC and BOD/COD because one is based on organic carbon while the other relies on two different types of oxygen demands. Since both BDOC and DOC are on the same basis (organic carbon), BDOC/DOC indicates the real biodegradability ratio. For example, BDOC/DOC of 0.20 means 20% of the DOC is biodegradable.

In addition to conventional Fenton reagent, which is catalyzed by ferrous iron (Fe^{2+}), modified Fenton reagents relying on ferric iron (Fe^{3+}) and zero-valent iron (Fe^{0}) as the catalysts have also been widely investigated for their abilities to degrade hazardous organic compounds [10–12]. The focuses of most studies have been on the compound disappearance and/or mineraliza-

* Corresponding author. Tel.: +1 701 231 7717; fax: +1 701 231 6185.
E-mail address: eakalak.khan@ndsu.edu (E. Khan).

0304-3894/$ – see front matter © 2008 Elsevier B.V. All rights reserved.
doi:10.1016/j.jhazmat.2008.04.049

tion. Different types of Fenton reagents were studied or compared on these attributes. They have not been compared on their abilities to increase biodegradability of organic contaminants, which is important if Fenton reaction is applied as a pretreatment prior to biological treatment. This study relied on the usefulness of BDOC/DOC to investigate the effect of iron type in Fenton reaction on the biodegradability enhancement of hazardous organics at low concentrations.

The main objective of this study was to compare the mineralization and biodegradability enhancement performances of traditional and modified Fenton reagents for the degradation of selected traditional and relatively new organic contaminants using DOC and BDOC/DOC as the indicators. The minor objectives were to examine the effects of iron and hydrogen peroxide doses, pH, and reaction time on the mineralization and biodegradability increase performances and to identify the oxidation by-products associated with each type of Fenton reagents. Trichloroethene (TCE), 2,4-dichlorophenol (2,4-DCP), 1,4-dioxane (1,4-D) and 1,2,3-trichloropropane (TCP) were the organic contaminants studied. All four compounds are classified by the United States Environmental Protection Agency as potential human carcinogens.

TCE and 2,4-DCP are traditional organic contaminants, which have been researched for their susceptibilities to Fenton degradation [13–18], but not on the comparison of biodegradability enhancement by different Fenton reagent types. Fe^0 can effectively reduce (dechlorinate) several chlorinated compounds including TCE and chlorophenols [19–22]. For 1,4-D and TCP, which are relatively new contaminants, the Fenton degradation of these two compounds has not been widely studied. There have been investigations on 1,4-D degradation by ultrasound with Fe^{2+} addition [23], Fenton reaction [24], and H_2O_2 + ultraviolet (UV) irradiation [25], and TCP degradation by Fenton reaction [26].

2. Materials and methods

2.1. Contaminant solution preparation

Analytical grade solutions of TCE, 2,4-DCP, 1,4-D and TCP (Sigma–Aldrich) were diluted with deionized (DI) water to prepare the contaminant solutions. The contaminant concentrations of the diluted solutions were 20 mg/L. All the diluted solutions were used in the conventional and modified Fenton oxidation experiments immediately after their preparations.

2.2. Experimental design and procedure

Three initial pHs of the Fenton reagents, 2–4, were examined. The selection of these pH values was based on the most effective pH range of 2–4 reported in previous studies for Fenton degradation of various organic contaminants [10,27–29]. To examine the effects of Fe and H_2O_2 doses on mineralization and biodegradability increase, three different Fe:H_2O_2:DOC ratios of 5:10:1, 10:10:1 [1], and 10:20:1 (mass basis) were applied. There was a total of 27 experiments (3 pH × 3 Fe:H_2O_2:DOC ratios × 3 Fe types) for each compound. All experiments were duplicated. The data presented in the next section (Section 3) were based on the averages of the duplicated experiments, of which the two data points were within ±3% of the averages in most cases.

Fenton oxidation was performed in a batch mode by using six 250 mL glass vials. The mixing was provided by a shaker (Ratex, Model DLS) at 180 rpm. All experiments were conducted at room temperature (25 ± 0.5 °C). After the contaminant solutions were prepared, their initial pHs were adjusted to the desired level by using either concentrated sulfuric acid (Merck, analytical grade) or sodium hydroxide (Merck, analytical grade). Then, 120 mL of the solutions were transferred into the reaction vials while 110 mL of the solutions were used for initial DOC and BDOC (DOC_0 and $BDOC_0$) measurements. The next step was the addition of ferrous sulfate (Sigma–Aldrich, analytical grade) into the vials, which were then sealed immediately with aluminum crimp caps and Teflon septa. Hydrogen peroxide (35%, Merck, analytical grade) was then added to the solution using a syringe via the septum. For the modified Fenton reagents, ferric chloride (Sigma–Aldrich, analytical grade) or iron powder (<10 μm, Merck) was added instead of ferrous sulfate. In the case of iron powder, after adding the powder, the contaminant solution was shaken for about 10 min before dosing H_2O_2. The shaking was to uniformly disperse iron powder in the solution while the time of 10 min was chosen arbitrarily.

After 5, 30, 60, 120, 180 and 240 min, the oxidation was terminated using 1 mL of a sodium thiosulfate solution to quench the residual H_2O_2 concentration in the vial. The solution of sodium thiosulfate was prepared by dissolving 23.7 g of sodium thiosulfate (Merck, analytical grade) in 100 mL DI water to make a concentration of 1.5 M. The amount of sodium thiosulfate added was 1.0, 1.2, 2.2, and 3.0 times of the stoichiometric requirements for the highest doses of H_2O_2 used in the degradation of 1,4-D, 2,4-DCP, TCP, and TCE, respectively. Although the stoichiometric requirements of sodium thiosulfate for all four contaminants were not the same because of different initial DOC concentrations (same initial concentrations as compound at 20 mg/L) and in turn different initial H_2O_2 concentrations, the same amount of sodium thiosulfate (1 mL of 1.5 M solution) was used for convenience. For the case of 1,4-D in which excess sodium thiosulfate was not provided, the stoichiometric amount should be adequate since results showed that the contaminant was substantially degraded (some of H_2O_2 was already used) at the first sampling time of 5 min (see Fig. 3a and b). Interferences of sodium thiosulfate on BDOC and DOC analyses have not been investigated but are unlikely since BDOC and DOC are based on the measurements of organic carbon.

The DOC, BDOC, and degradation by-products were monitored with reaction time by sacrificing one of the six vials at each time. Ten milliliters of the mixture from the vial were used for DOC (DOC at time t or DOC_t) measurement while the remaining was used for BDOC (BDOC at time t or $BDOC_t$) and by-product analyses. Degradation by-products were measured only at 240 min of reaction time. It should be noted that pH changes during the degradation were minimal (±0.3).

2.3. Analytical methods

BDOC was determined following the procedure of Khan et al. [9]. The sample was adjusted to pH of 6.5–7.5 with concentrated sodium hydroxide. Then, the sample was filtered through a 0.7-μm glass fiber filter (GF/F, Whatman), and measured for DOC. Next, the sample was placed in a 100-mL vial. One milliliter of mixed liquor collected from an aeration tank of a brewery wastewater treatment plant was added as an inoculum to the vial. The ranges of suspended solids and volatile suspended solids concentrations of the mixed liquor used in this study were 950–1200 mg/L and 700–1050 mg/L, respectively. The mixture in the vial was incubated at 20 °C for 5 days. After the incubation, DOC was measured again. A blank control was included by using DI water as a sample. The difference in DOC reduction of the sample and the blank during the incubation was BDOC. DOC was analyzed using a total organic carbon analyzer (Shimadzu, Model 5000A) after the samples were filtered through a 0.7-μm glass fiber filter (GF/F, Whatman). The degradation by-products were analyzed using a gas chromatograph/mass spectrometer (Thermo Finnigan) with a ZB-5 column

Table 1
DOC elimination, biodegradability increase, and refractory fractions at the reaction time of 120 min and initial biodegradability of the TCE solution for all experimental conditions

Fe type	Fe:H_2O_2:DOC	pH	Fraction			
			DOC elimination	Initial biodegradability	Biodegradability increase	Refractory
Fe^{2+}	10:10:1	2	0.39	0.06	0.21	0.34
		3	0.48	0.06	0.19	0.27
		4	0.43	0.05	0.25	0.27
	10:20:1	2	0.42	0.03	0.25	0.30
		3	0.50	0.06	0.19	0.25
		4	0.45	0.06	0.24	0.25
	5:10:1	2	0.44	0.01	0.25	0.30
		3	0.56	0.05	0.16	0.23
		4	0.53	0.05	0.20	0.22
Fe^{3+}	10:10:1	2	0.35	0.05	0.28	0.32
		3	0.38	0.03	0.26	0.33
		4	0.40	0.03	0.25	0.32
	10:20:1	2	0.37	0.05	0.26	0.32
		3	0.36	0.03	0.26	0.35
		4	0.43	0.04	0.21	0.32
	5:10:1	2	0.38	0.06	0.22	0.34
		3	0.43	0.03	0.22	0.32
		4	0.43	0.05	0.20	0.32
Fe^0	10:10:1	2	0.36	0.03	0.25	0.36
		3	0.40	0.04	0.24	0.32
		4	0.31	0.04	0.24	0.41
	10:20:1	2	0.41	0.03	0.23	0.33
		3	0.46	0.06	0.22	0.26
		4	0.38	0.03	0.23	0.36
	5:10:1	2	0.39	0.06	0.24	0.31
		3	0.42	0.06	0.24	0.28
		4	0.35	0.04	0.26	0.35

(Phenomenex). pH was measured using a pH meter (Hach, Model EC-30).

3. Results and discussion

3.1. General degradation trends

The mineralization of all four compounds indicated by DOC elimination fraction occurred mostly in 120 min for almost all conditions. The DOC elimination fraction at 120 min was more than 90% of that at 240 min. The exceptions were the cases of Fe^{2+} and Fe^{3+} for TCP degradation, which more than 90% of the DOC elimination fraction at 240 min was reached at 180 min. The DOC elimination fraction is defined according to the following equation:

$$\text{DOC elimination fraction} = \frac{\text{DOC}_0 - \text{DOC}_t}{\text{DOC}_0} \quad (1)$$

where DOC_0 = DOC at reaction time = 0 min or initial DOC and DOC_t = DOC at reaction time = t min.

The biodegradability increase approached completion after only 60 min based on a similar justification that the biodegradability increase fraction at 60 min was more than 90% of that at 240 min. The biodegradability increase fraction is defined as

$$\text{Biodegradability increase fraction} = \frac{\text{BDOC}_t}{\text{DOC}_0} - \frac{\text{BDOC}_0}{\text{DOC}_0} \quad (2)$$

$$\text{Biodegradability increase fraction} = \frac{\text{BDOC}_t - \text{BDOC}_0}{\text{DOC}_0} \quad (3)$$

where $BDOC_0$ = BDOC at reaction time = 0 min or initial BDOC, and $BDOC_t$ = BDOC at reaction time = t min.

These results indicate that during the first 60 min some of the contaminants were both mineralized and partially degraded to more biodegradable products while between 60 and 120 min, the contaminants were only mineralized. In addition, the overall reaction time required was controlled by the reaction times for mineralization to approach completion of 120 min for TCE, 2,4-DCP, and 1,4-D and 180 min for TCP.

3.2. Effects of iron type, Fe:H_2O_2:DOC ratio (Fe and H_2O_2 doses), and pH on mineralization and biodegradability increase performances

3.2.1. TCE

The DOC elimination, biodegradability increase and refractory fractions at the reaction time of 120 min, and initial biodegradability of the TCE solution for all experimental conditions are shown in Table 1. The refractory fraction was determined based on the following mass balance:

$$\text{DOC elimination fraction} + \text{biodegradability increase fraction} + \text{initial biodegradability fraction} + \text{refractory fraction} = 1.00 \quad (4)$$

The initial biodegradability fraction is defined as

$$\text{Initial biodegradability fraction} = \frac{\text{BDOC}_0}{\text{DOC}_0} \quad (5)$$

Substituting Eqs. (1), (3), and (5) in Eq. (4) results in

$$\text{Refractory fraction} = \frac{\text{DOC}_t - \text{BDOC}_t}{\text{DOC}_0} \quad (6)$$

As an example, the experimental results for Fe^{2+}, Fe:H_2O_2:DOC ratio of 5:10:1, and pH 2 are as follows: DOC_0 = 3.05 mg/L, DOC_{120} = 1.86 mg/L, $BDOC_0$ = 0.18 mg/L, $BDOC_{120}$ = 0.83 mg/L. Substituting these DOC and BDOC values in Eqs. (1), (3), and (5) results in DOC elimination fraction = 0.39, biodegradability increase fraction = 0.21, and initial biodegradability fraction = 0.06, respectively. Based on these values and Eq. (4), refractory fraction = 0.34. Alternatively, the refractory fraction can be calculated by substituting DOC_{120}, $BDOC_{120}$, and DOC_0 values in Eq. (6).

Table 2
DOC elimination, biodegradability increase, and refractory fractions at the reaction time of 120 min and initial biodegradability of the 2,4-DCP solution for all experimental conditions

Fe type	$Fe:H_2O_2:DOC$	pH	Fraction			
			DOC elimination	Initial biodegradability	Biodegradability increase	Refractory
		2	0.34	0.04	0.17	0.45
	5:10:1	3	0.36	0.05	0.18	0.41
		4	0.39	0.04	0.18	0.39
		2	0.34	0.05	0.20	0.41
Fe^{2+}	10:10:1	3	0.37	0.05	0.22	0.36
		4	0.37	0.05	0.24	0.34
		2	0.35	0.04	0.27	0.34
	10:20:1	3	0.38	0.04	0.28	0.30
		4	0.43	0.05	0.27	0.25
		2	0.31	0.04	0.16	0.49
	5:10:1	3	0.33	0.05	0.20	0.42
		4	0.34	0.05	0.18	0.43
		2	0.34	0.03	0.21	0.42
Fe^{3+}	10:10:1	3	0.36	0.05	0.23	0.36
		4	0.39	0.04	0.21	0.36
		2	0.38	0.05	0.22	0.35
	10:20:1	3	0.40	0.04	0.25	0.31
		4	0.42	0.04	0.23	0.31
Fe^0		2	0.37	0.04	0.31	0.28
	5:10:1	3	0.34	0.04	0.29	0.33
		4	0.32	0.06	0.27	0.35
		2	0.41	0.04	0.30	0.25
	10:10:1	3	0.38	0.05	0.28	0.29
		4	0.36	0.04	0.26	0.34
		2	0.44	0.05	0.30	0.21
	10:20:1	3	0.42	0.05	0.29	0.24
		4	0.39	0.06	0.28	0.27

The values of initial biodegradability fraction of TCE ranged from 0.01 to 0.06. This indicates the biorecalcitrant nature of the compound if no or minimal TCE microbial degraders are present. Although the biodegradability increase fraction was the highest at $Fe^{3+}:H_2O_2$:DOC of 5:10:1 and pH 2, the other conditions also provided comparable results except for a few cases with Fe^{2+}. The biodegradability increases from between 0.01 and 0.06 to between 0.17 and 0.28 were not dramatic but these increases occurred while 35–55% of the compound was mineralized. Fe^{2+} provided the highest mineralization fraction compared with Fe^{3+} and Fe^0 at the same pH and $Fe:H_2O_2$:DOC ratio. The DOC elimination fraction was distinctively higher at the highest Fe^{2+} and H_2O_2 doses ($Fe:H_2O_2$:DOC ratio of 10:20:1) and higher pH (3 and 4). This domination resulted in the two least refractory fractions (0.23 and 0.22) at these conditions. For Fe^{3+} and Fe^{0+}, the effects of pH and $Fe:H_2O_2$:DOC on both mineralization and biodegradability increase fractions were not pronounced. As a consequence, the refractory fractions at different conditions for these two Fe types were not much different.

3.2.2. 2,4-DCP

Table 2 presents the DOC elimination, biodegradability increase, and refractory fractions at the reaction time of 120 min, and initial biodegradability of the 2,4-DCP solution for all experimental conditions. The initial biodegradability fractions were low ranging from 0.03 to 0.06. The biodegradability increase fractions were between 0.16 and 0.31 and 4–8 times of the initial biodegradability. Although the range of biodegradability increase fraction was quite small, the superiority of Fe^0 over Fe^{2+} and Fe^{3+} in enhancing the biodegradability was evident. Unlike the results of TCE, Fe^{2+} did not provide higher mineralization fractions. $Fe:H_2O_2$:DOC ratio rather than the Fe type had a noticeable effect on the degree of mineralization. For each Fe type, at the same pH, the largest mineralization faction occurred at the highest $Fe:H_2O_2$:DOC ratio. As a result, the two least refractory fractions (0.21 and 0.24) were observed at $Fe^0:H_2O_2$:DOC ratio of 10:20:1 at pH 2 and 3. It should be noted comparable refractory fractions were also obtainable at $Fe^0:H_2O_2$:DOC ratio of 10:20:1 at pH 4, $Fe^0:H_2O_2$:DOC ratio of 10:10:1 at pH 2, and $Fe^{2+}:H_2O_2$:DOC ratio of 10:20:1 at pH 4.

3.2.3. 1,4-D

Table 3 presents the DOC elimination, biodegradability increase, and refractory fractions at the reaction time of 120 min, and initial biodegradability of the 1,4-D solution for all experimental conditions. The initial biodegradability fractions of 0.03–0.04 indicated the biorefractory nature of 1,4-D prior to Fenton reaction. The fraction of DOC elimination was less than 0.10 in all cases. Unlike the above two traditional contaminants, 1,4-D was not susceptible to Fenton reaction in term of mineralization. However, the range of biodegradability increase fraction was from 0.28 to 0.58, much higher than the values observed for TCE and 2,4-DCP. This suggests that Fenton reaction was capable of degrading 1,4-D to biodegradable products rather than CO_2. Using Fe^{2+} resulted in slightly more mineralization fraction. In addition, the $Fe^{2+}:H_2O_2$:DOC ratio of 10:20:1 was favorable for increasing biodegradability fraction. For Fe^{3+} and Fe^0, $Fe:H_2O_2$:DOC ratio and pH did not substantially affect mineralization while higher $Fe:H_2O_2$:DOC ratios were better for biodegradability increase with $Fe:H_2O_2$:DOC ratio of 10:10:1 superior to that of 10:20:1.

3.2.4. TCP

Table 4 shows the DOC elimination, biodegradability increase, and refractory fractions at the reaction time of 180 min, and initial biodegradability of the TCP solution for all experimental conditions. Same as the first three contaminants, the initial biodegradability fraction was low ranging between 0.03 and 0.05. Similar to

Table 3
DOC elimination, biodegradability increase, and refractory fractions at the reaction time of 120 min and initial biodegradability of the 1,4-D solution for all experimental conditions

Fe type	$Fe:H_2O_2:DOC$	pH	Fraction			
			DOC elimination	Initial biodegradability	Biodegradability increase	Refractory
Fe^{2+}	5:10:1	2	0.06	0.03	0.31	0.60
		3	0.08	0.04	0.37	0.51
		4	0.07	0.03	0.33	0.57
	10:10:1	2	0.08	0.04	0.39	0.49
		3	0.09	0.04	0.47	0.40
		4	0.08	0.04	0.42	0.46
	10:20:1	2	0.08	0.03	0.49	0.40
		3	0.10	0.04	0.58	0.28
		4	0.09	0.04	0.51	0.36
Fe^{3+}	5:10:1	2	0.02	0.04	0.36	0.58
		3	0.04	0.04	0.29	0.63
		4	0.03	0.03	0.28	0.66
	10:10:1	2	0.03	0.04	0.54	0.39
		3	0.05	0.04	0.47	0.44
		4	0.04	0.04	0.45	0.47
	10:20:1	2	0.04	0.04	0.50	0.42
		3	0.05	0.04	0.46	0.45
		4	0.04	0.04	0.45	0.47
Fe^{0}	5:10:1	2	0.03	0.03	0.37	0.57
		3	0.03	0.03	0.41	0.53
		4	0.04	0.03	0.38	0.55
	10:10:1	2	0.05	0.04	0.45	0.46
		3	0.06	0.03	0.52	0.39
		4	0.05	0.04	0.47	0.44
	10:20:1	2	0.04	0.04	0.39	0.53
		3	0.05	0.04	0.46	0.45
		4	0.05	0.04	0.41	0.50

the results of TCE, the biodegradability increase fractions for different conditions were in a narrow range and Fe^{2+} was the most effective in mineralization especially at $Fe:H_2O_2$:DOC of 10:10:1. The main differences between the results of TCE and TCP were that Fe^{0} was also effective in mineralization and the highest $Fe:H_2O_2$:DOC ratio was not necessarily the best condition. Again, no trend can be established between pH and the effectiveness of both mineralization and biodegradability increase. The least refractory fraction observed at the favorable conditions was approximately 25%.

Table 4
DOC elimination, biodegradability increase, and refractory fractions at the reaction time of 180 min and initial biodegradability of the TCP solution for all experimental conditions

Fe type	$Fe:H_2O_2:DOC$	pH	Fraction			
			DOC elimination	Initial biodegradability	Biodegradability increase	Refractory
Fe^{2+}	5:10:1	2	0.33	0.05	0.21	0.41
		3	0.39	0.03	0.22	0.36
		4	0.36	0.04	0.24	0.36
	10:10:1	2	0.39	0.04	0.29	0.28
		3	0.44	0.04	0.27	0.25
		4	0.41	0.05	0.30	0.24
	10:20:1	2	0.33	0.04	0.29	0.34
		3	0.36	0.04	0.28	0.32
		4	0.33	0.04	0.32	0.31
Fe^{3+}	5:10:1	2	0.29	0.05	0.20	0.46
		3	0.31	0.04	0.23	0.42
		4	0.28	0.04	0.26	0.42
	10:10:1	2	0.28	0.03	0.28	0.41
		3	0.34	0.04	0.28	0.34
		4	0.30	0.03	0.34	0.33
	10:20:1	2	0.31	0.04	0.30	0.35
		3	0.35	0.04	0.32	0.29
		4	0.31	0.05	0.34	0.30
Fe^{0}	5:10:1	2	0.37	0.05	0.28	0.30
		3	0.33	0.05	0.25	0.37
		4	0.32	0.05	0.27	0.36
	10:10:1	2	0.40	0.04	0.32	0.24
		3	0.36	0.05	0.27	0.32
		4	0.33	0.05	0.31	0.31
	10:20:1	2	0.38	0.05	0.30	0.27
		3	0.34	0.05	0.27	0.34
		4	0.32	0.05	0.31	0.32

3.2.5. Comparison of the results of the four compounds studied

Using the least refractory fraction as a criterion, Fe^{2+} was the most suitable iron type for the degradation of TCE, 1,4-D, and TCP while Fe^0 was the best for 2,4-DCP degradation. Fenton reaction mineralized more than increased the biodegradability of TCE, 2,4-DCP, and TCP. The effects of Fenton reaction on 1,4-D mineralization and biodegradability increase was the opposite. The ranges of the least refractory fractions of the TCE, 2,4-DCP, and TCP were between 0.20 and 0.25 while those of 1,4-D were from 0.28 to 0.40. These results suggest that 1,4-D was more recalcitrant to Fenton degradation than the other three compounds. Higher $Fe:H_2O_2$:DOC ratios were better conditions with the ratio of 10:20:1 being the best for TCE, 2,4-DCP, and 1,4-D and the ratio of 10:10:1 being the most effective for TCP. TCP required smaller H_2O_2 doses than the other compounds, although the final performances were not necessarily better. For all four compounds, there was no trend between pH and the magnitudes of mineralization and biodegradability increase. This may be because of the narrow range of pH studied which is known to be a suitable range for Fenton degradation [10,27–29].

3.3. Degradation kinetics

It is not possible to present the DOC and BDOC evolutions with time for all 27 conditions (a total of 54 curves for each compound). Therefore, only the DOC and BDOC transient curves of the Fe type and $Fe:H_2O_2$:DOC ratio that provided the least refractory fraction for each compound are shown here as examples. Fig. 1 shows DOC normalized by initial DOC (DOC_t/DOC_0) and BDOC normalized by initial DOC ($BDOC_t/DOC_0$) versus time (a and b) and the kinetic fittings of the DOC data and BDOC data (c and d) of the TCE solution for $Fe^{2+}:H_2O_2$:DOC of 10:20:1. The error bars in Fig. 1a and b are the differences between the duplicated experiments. As mentioned above, DOC elimination was complete after 120 min (Fig. 1a) while biodegradability increase occurred mostly within the first 60 min. Subtracting the data in Fig. 1a from 1.00 results in the mineralization fraction. The data in Fig. 1b minus initial biodegradability ($BDOC_0/DOC_0$) equals to the biodegradability increase fraction. The first-order and zero-order kinetic models were the best for describing the DOC and BDOC data in Fig. 1a and b, respectively (Fig. 1c and d). It should be noted that only the DOC data up to 120 min and the BDOC data up to 60 min were used for the kinetic fittings since there were no or minimal changes in the data after these times. In addition, only zero- to second-order models were considered.

Figs. 2–4 present the same types of data as Fig. 1 for the 2,4-DCP, 1,4-D, and TCP solutions, respectively. The error bars visually interfere with the data and are not included in these figures. As mentioned in Section 2, the differences in results of the duplicated experiments were within ±3%. For the TCP solution, the least refractory fraction of 0.24 was obtained at $Fe^0:H_2O_2$:DOC of 10:10:1 and $Fe^{2+}:H_2O_2$:DOC of 10:10:1 (Table 4) but the data at the latter condition are shown in Fig. 4 because it provided consistently low refractory fractions across all three pH values. Figs. 2–4 show that pH within the range studied had minimal effects on mineralization and biodegradability enhancement. For the TCP solution, small BDOC decreases after 60 min might be because of the mineralization of biodegradable by-products (BDOC contributing compounds). The zero-order model was better than the other models considered in describing the BDOC data of all three compounds. The DOC data followed the first-order model for 1,4-D and TCP but the second-order model for 2,4-DCP.

Tables 5–8 summarize the kinetic constants and coefficients of determination (r^2) of the fittings for all four compounds and experimental conditions. The kinetics of DOC reduction followed the first-order model for all four compounds when Fe^{2+} and Fe^{3+} were used. Fe^0 catalyzed Fenton degradation agreed with the second-order kinetics for TCE, 2,4-DCP, and TCP and the first-order kinetics for 1,4-D. Among the kinetic models tested, the BDOC increase kinetics of all four compounds and conditions matched the zero-order model the most. The r^2 of the DOC reduction and BDOC increase kinetic fits were more than 0.85 and 0.70, respectively, in most cases. Although the r^2 values were low (0.3–0.5) in some cases, the fittings by the other kinetic models would give even lower r^2. There might be an existing kinetic model or it is possible to develop one that would describe the data better. However, such an effort is beyond the scope of this study. The higher amount of iron tended to increase DOC reduction rate but had less influence on the rate of BDOC increase. There were no clear trends between pH magnitude and the kinetics of mineralization and biodegradability increase. The H_2O_2 amount affected less cases of both kinetics compared to the iron amount.

3.4. Degradation by-products

All four contaminants were not detectable after 240 min. This suggests that the refractory fractions shown in Tables 1–4 were mostly degradation by-products that were not biodegradable. Table 9 presents degradation by-products observed at the end of the Fenton reactions catalyzed by different types of iron. The degradation by-products from Fenton reactions using Fe^{2+} and Fe^{3+} were different than those from Fenton reactions using Fe^0 except for the degradation of 1,4-D. Phosgene and dichloroacetyl chloride were the by-products obtained from Fe^{2+} and Fe^{3+} catalyzed Fenton degradation of TCE. The same by-products generated in Fenton reaction using Fe^{2+} and Fe^{3+} were due to the similar oxidation mechanism of TCE by the attack of $OH^\bullet$ [30]. Ethene, ethane, and vinyl chloride were found for the case of Fe^0 based Fenton reaction. The observation of these by-products was because Fenton reaction catalyzed by Fe^0 results in not only oxidation but also reduction. The corrosion of Fe^0 releases Fe^{2+} (which will further react with H_2O_2) and electrons into the solution [19]. Then, the electrons transfer to the compound (TCE) leads to the replacement of a chlorine atom with a hydrogen atom and liberation of chloride ion [19].

For Fe^{2+} and Fe^{3+} catalyzed Fenton degradation of 2,4-DCP, detected by-products were chlorohydroquinone, 2-chloro-1,4-benzoquinone and 4,6-dichlororesorcinol. These compounds were reported as the major intermediates of the photo Fenton-like oxidation of 2,4-DCP [18]. When Fe^0 was used, hydroquinone and catechol were observed. The reason for having different by-products with Fe^0 is the same as described above for TCE degradation.

Unlike the first two contaminants, 1,4-D degradation by-products were the same regardless of the iron type. Several previous studies on advanced oxidation (TiO_2 photocatalysis, UV/H_2O_2 and O_3/H_2O_2) of 1,4-D found 1,2-ethanediol diformate as a major by-product [31–33]. In this study, 1,2-ethanediol monoformate, formic acid, and methoxyacetic acid were the by-products obtained in addition to 1,2-ethanediol diformate. These compounds are known to be more biodegradable compared to the other by-products listed in Table 9. This explains the finding presented above on why Fenton degradation of 1,4-D resulted in more biodegradability increase and less mineralization. Kim et al. [25] also reported readily biodegradable organic acids such as acetic, propionic, and butyric, as intermediates of photo-Fenton degradation of 1,4-D.

Four main by-products, 1,3-dichloro-2-propanone, 2,3-dichloro-1-propene, isopropanol, and propionic aldehyde, were identified for the Fenton degradation of TCP. When Fe^{2+} and Fe^{3+} were used, 1,3-dichloro-2-propanone and 2,3-dichloro-1-propene were detected. 1,3-Dichloro-2-propanone was previously reported as a by-product of the standard Fenton degradation of TCP [26]. For Fe^0, isopropanol and propionic aldehydes were the by-products.

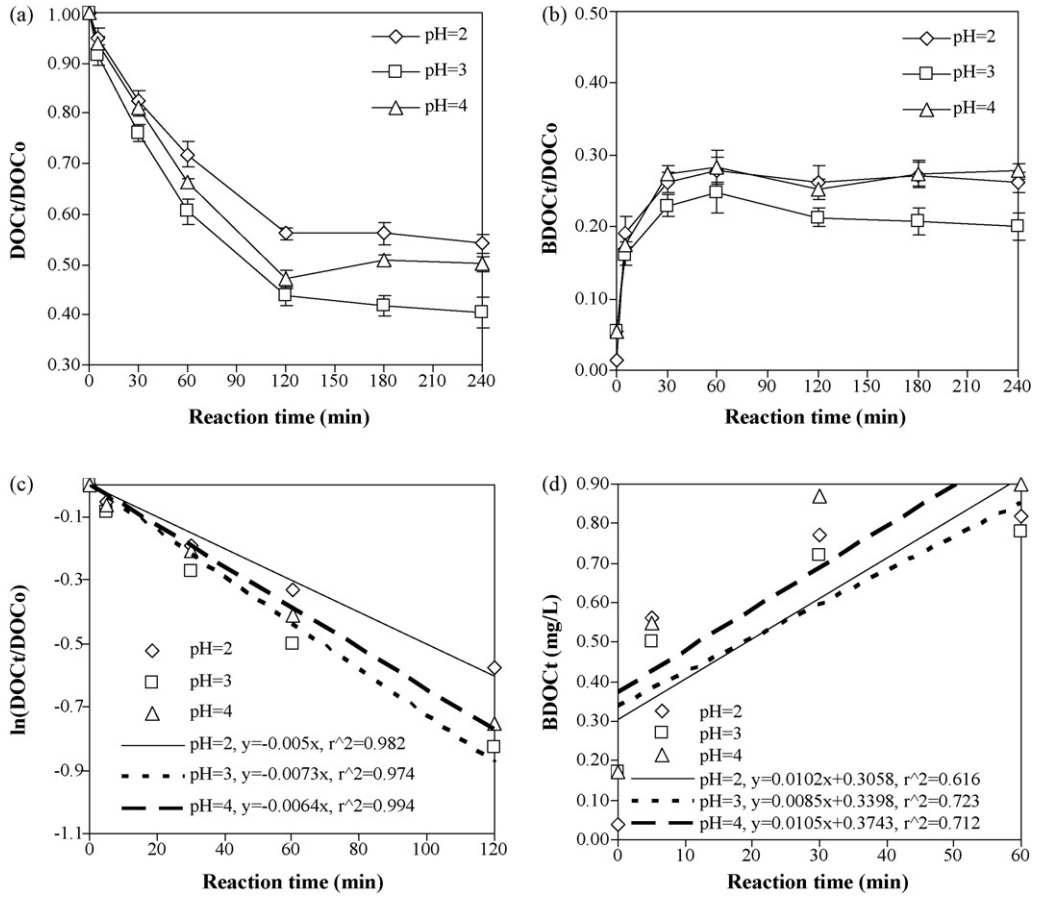

Fig. 1. (a) Normalized DOC versus reaction time, (b) normalized BDOC versus reaction time, (c) first-order kinetics fitting of DOC reduction, and (d) zero-order fitting of BDOC increase of the TCE solution for Fe^{2+}:H_2O_2:DOC of 10:20:1.

Table 5
DOC reduction and BDOC increase kinetic constants, and r^2 of the kinetic fittings of the TCE solution for all experimental conditions

Fe type	Fe:H_2O_2:DOC	pH	DOC reduction		BDOC increase	
			Kinetic constant	r^2	Kinetic constant (mg/L min)	r^2
Fe^{2+}	5:10:1	2	0.0042 min^{-1}	0.987	0.0110	0.777
		3	0.0054 min^{-1}	0.999	0.0100	0.769
		4	0.0047 min^{-1}	0.995	0.0133	0.777
	10:10:1	2	0.0052 min^{-1}	0.889	0.0092	0.642
		3	0.0064 min^{-1}	0.934	0.0074	0.558
		4	0.0056 min^{-1}	0.906	0.0094	0.641
	10:20:1	2	0.0050 min^{-1}	0.982	0.0102	0.616
		3	0.0073 min^{-1}	0.974	0.0085	0.723
		4	0.0064 min^{-1}	0.994	0.0105	0.712
Fe^{3+}	5:10:1	2	0.0034 min^{-1}	0.952	0.0131	0.725
		3	0.0045 min^{-1}	0.943	0.0111	0.604
		4	0.0050 min^{-1}	0.992	0.0096	0.623
	10:10:1	2	0.0038 min^{-1}	0.997	0.0143	0.928
		3	0.0042 min^{-1}	0.995	0.0119	0.908
		4	0.0047 min^{-1}	0.970	0.0115	0.835
	10:20:1	2	0.0039 min^{-1}	0.978	0.0122	0.938
		3	0.0042 min^{-1}	0.973	0.0122	0.786
		4	0.0056 min^{-1}	0.984	0.0100	0.809
Fe^0	5:10:1	2	0.0028 L/min mg	0.892	0.0082	0.375
		3	0.0029 L/min mg	0.887	0.0090	0.394
		4	0.0023 L/min mg	0.851	0.0074	0.393
	10:10:1	2	0.0031 L/min mg	0.918	0.0080	0.322
		3	0.0038 L/min mg	0.927	0.0069	0.308
		4	0.0029 L/min mg	0.950	0.0075	0.339
	10:20:1	2	0.0028 L/min mg	0.883	0.0102	0.553
		3	0.0032 L/min mg	0.885	0.0106	0.583
		4	0.0034 L/min mg	0.881	0.0109	0.646

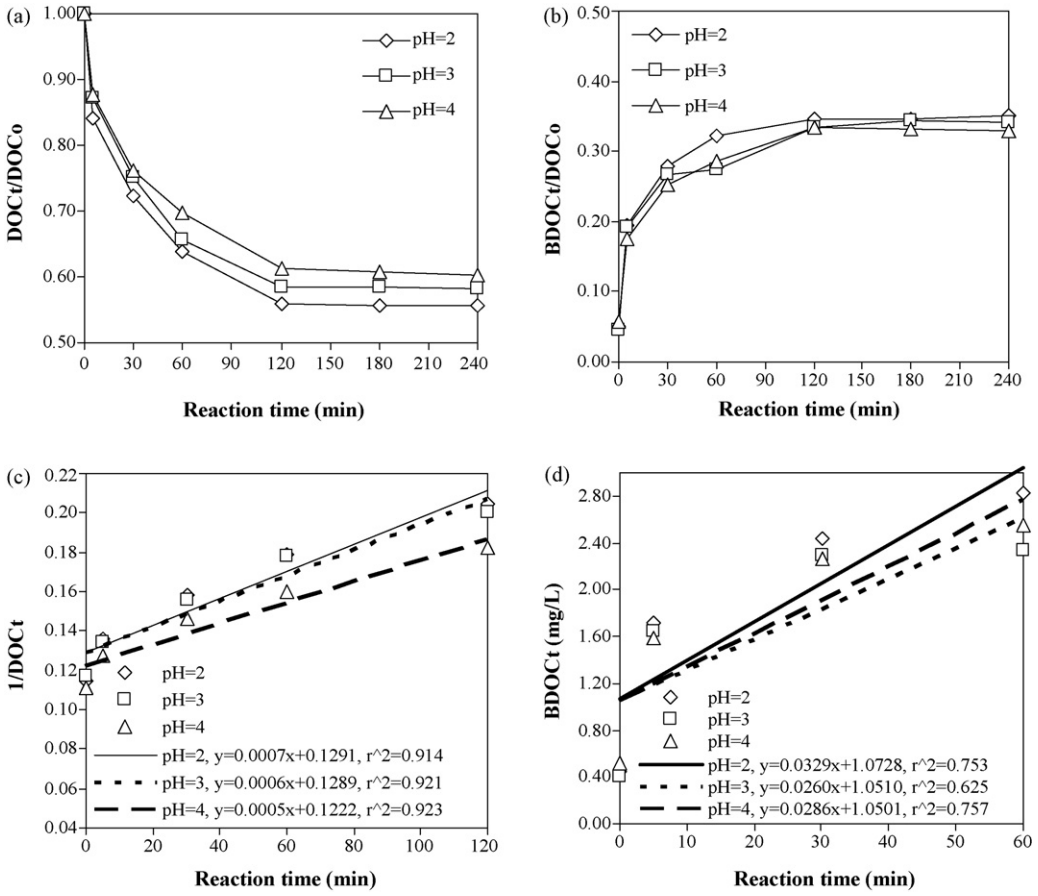

Fig. 2. (a) Normalized DOC versus reaction time, (b) normalized BDOC versus reaction time, (c) second-order kinetics fitting of DOC reduction, and (d) zero-order fitting of BDOC increase of the 2,4-DCP solution for Fe^0:H_2O_2:DOC of 10:20:1.

Table 6
DOC reduction and BDOC increase kinetic constants, and r^2 of the kinetic fittings of the 2,4-DCP solution for all experimental conditions

Fe type	Fe:H_2O_2:DOC	pH	DOC reduction		BDOC increase	
			Kinetic constant	r^2	Kinetic constant (mg/L min)	r^2
	5:10:1	2	0.0035 min^{-1}	0.990	0.0161	0.579
		3	0.0042 min^{-1}	0.974	0.0192	0.620
		4	0.0046 min^{-1}	0.960	0.0198	0.552
	10:10:1	2	0.0046 min^{-1}	0.973	0.0176	0.628
Fe^{2+}		3	0.0056 min^{-1}	0.988	0.0217	0.557
		4	0.0053 min^{-1}	0.983	0.0235	0.550
	10:20:1	2	0.0046 min^{-1}	0.986	0.0241	0.596
		3	0.0051 min^{-1}	0.981	0.0277	0.569
		4	0.0066 min^{-1}	0.991	0.0262	0.533
		2	0.0021 min^{-1}	0.973	0.0193	0.747
	5:10:1	3	0.0025 min^{-1}	0.979	0.0259	0.707
		4	0.0028 min^{-1}	0.952	0.0224	0.659
		2	0.0028 min^{-1}	0.991	0.0206	0.570
Fe^{3+}	10:10:1	3	0.0029 min^{-1}	0.988	0.0280	0.700
		4	0.0034 min^{-1}	0.983	0.0249	0.689
		2	0.0033 min^{-1}	0.995	0.0279	0.716
	10:20:1	3	0.0040 min^{-1}	0.999	0.0342	0.731
		4	0.0043 min^{-1}	0.998	0.0294	0.688
Fe^0	5:10:1	2	0.0005 L/min mg	0.906	0.0322	0.775
		3	0.0005 L/min mg	0.893	0.0257	0.785
		4	0.0004 L/min mg	0.931	0.0255	0.875
	10:10:1	2	0.0006 L/min mg	0.894	0.0303	0.700
		3	0.0006 L/min mg	0.923	0.0277	0.757
		4	0.0005 L/min mg	0.914	0.0267	0.744
	10:20:1	2	0.0007 L/min mg	0.914	0.0329	0.753
		3	0.0006 L/min mg	0.921	0.0260	0.625
		4	0.0005 L/min mg	0.923	0.0286	0.757

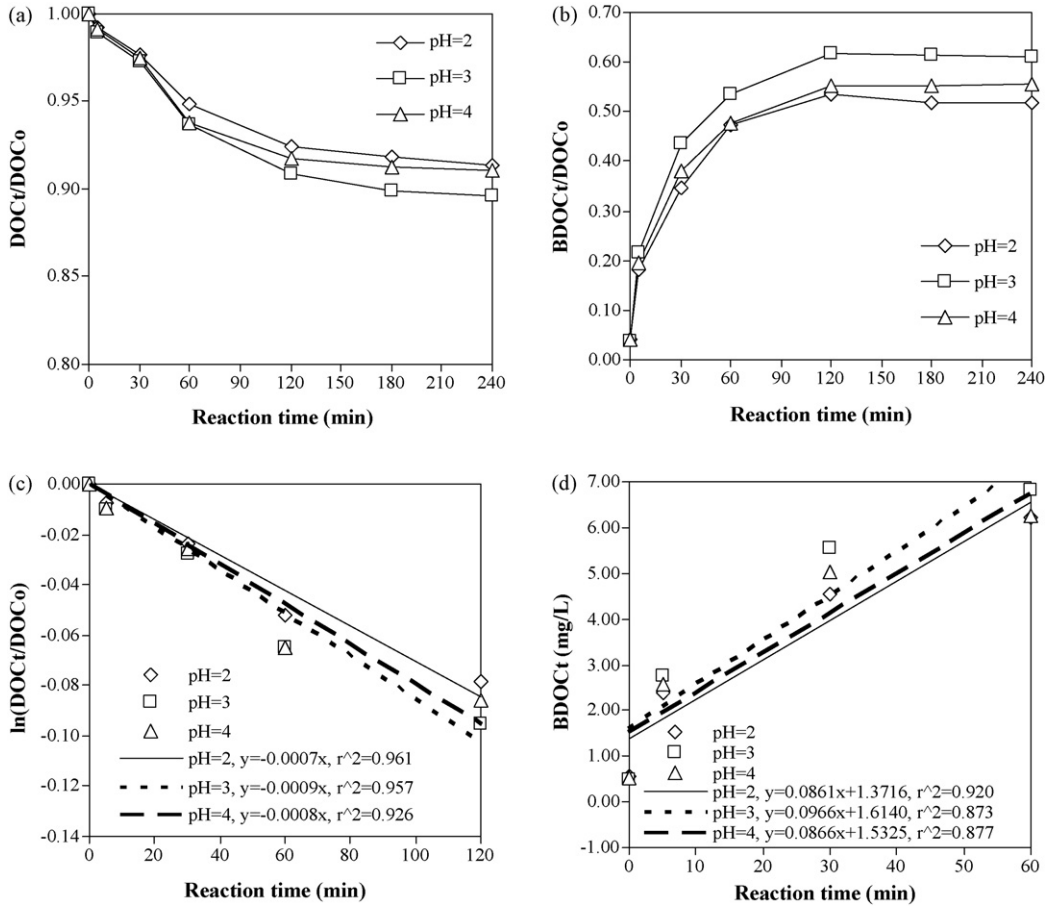

Fig. 3. (a) Normalized DOC versus reaction time, (b) normalized BDOC versus reaction time, (c) first-order kinetics fitting of DOC reduction, and (d) zero-order fitting of BDOC increase of the 1,4-D solution for Fe^{2+}:H_2O_2:DOC of 10:20:1.

Table 7
DOC reduction and BDOC increase kinetic constants, and r^2 of the kinetic fittings of the 1,4-D solution for all experimental conditions

Fe type	Fe:H_2O_2:DOC	pH	DOC reduction		BDOC increase	
			Kinetic constant (min^{-1})	r^2	Kinetic constant (mg/L min)	r^2
Fe^{2+}	5:10:1	2	0.0005	0.930	0.0507	0.890
		3	0.0007	0.978	0.0671	0.883
		4	0.0006	0.957	0.0503	0.868
	10:10:1	2	0.0007	0.966	0.0628	0.951
		3	0.0008	0.958	0.0777	0.899
		4	0.0008	0.904	0.0653	0.906
	10:20:1	2	0.0007	0.961	0.0861	0.920
		3	0.0009	0.957	0.0966	0.873
		4	0.0008	0.926	0.0866	0.877
Fe^{3+}	5:10:1	2	0.0002	0.851	0.0635	0.986
		3	0.0003	0.983	0.0521	0.984
		4	0.0003	0.959	0.0398	0.968
	10:10:1	2	0.0002	0.833	0.1008	0.981
		3	0.0005	0.891	0.0856	0.986
		4	0.0004	0.903	0.0726	0.983
	10:20:1	2	0.0003	0.898	0.0841	0.977
		3	0.0004	0.921	0.0701	0.980
		4	0.0004	0.800	0.0564	0.968
Fe^{0}	5:10:1	2	0.0003	0.612	0.0652	0.975
		3	0.0003	0.546	0.0772	0.924
		4	0.0004	0.435	0.0737	0.941
	10:10:1	2	0.0005	0.864	0.0825	0.967
		3	0.0006	0.721	0.1010	0.942
		4	0.0005	0.716	0.0832	0.953
	10:20:1	2	0.0004	0.349	0.0715	0.930
		3	0.0005	0.685	0.0954	0.950
		4	0.0005	0.495	0.0770	0.919

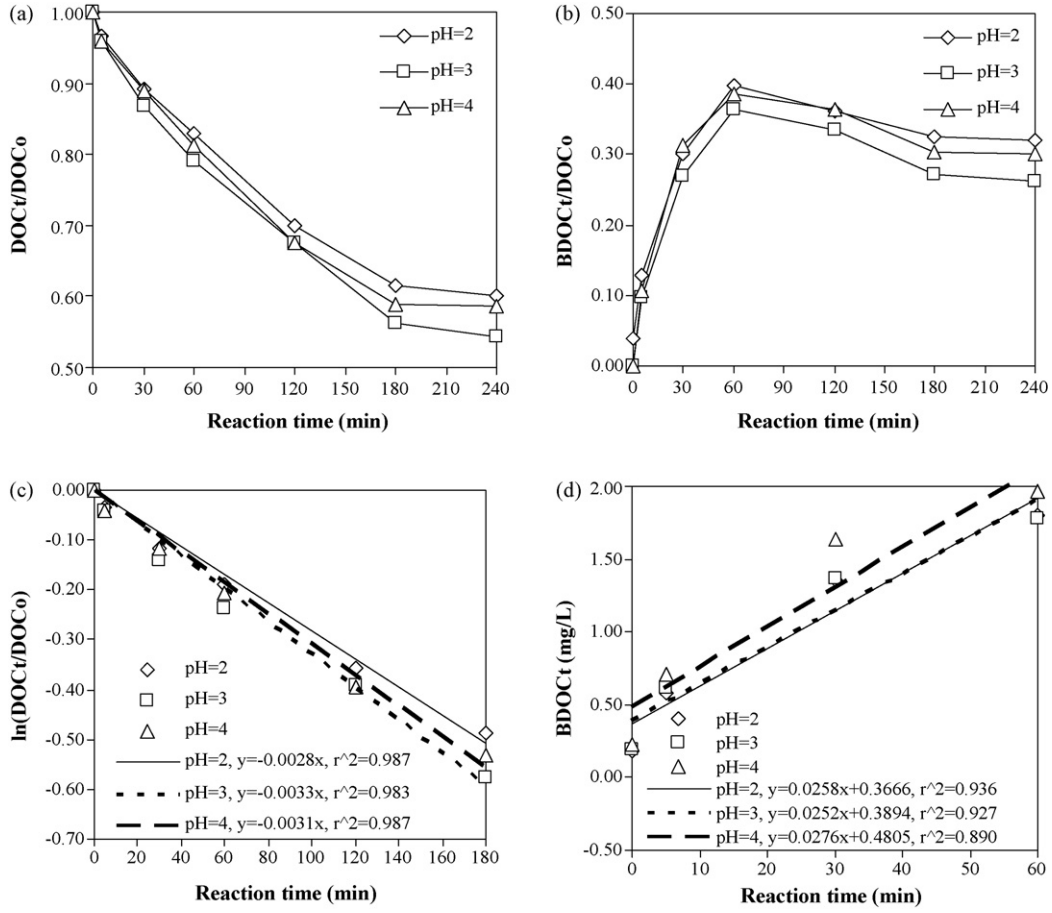

Fig. 4. (a) Normalized DOC versus reaction time, (b) normalized BDOC versus reaction time, (c) first-order kinetics fitting of DOC reduction, and (d) zero-order fitting of BDOC increase of the TCP solution for Fe^{2+}:H_2O_2:DOC of 10:10:1.

Table 8
DOC reduction and BDOC increase kinetic constants, and r^2 of the kinetic fittings of the TCP solution for all experimental conditions

Fe type	Fe:H_2O_2:DOC	pH	DOC reduction		BDOC increase	
			Kinetic constant	r^2	Kinetic constant (mg/L min)	r^2
Fe^{2+}	5:10:1	2	0.0023 min^{-1}	0.995	0.0179	0.948
		3	0.0028 min^{-1}	0.992	0.0188	0.897
		4	0.0026 min^{-1}	0.990	0.0200	0.843
	10:10:1	2	0.0028 min^{-1}	0.987	0.0258	0.936
		3	0.0033 min^{-1}	0.983	0.0252	0.927
		4	0.0031 min^{-1}	0.987	0.0276	0.890
	10:20:1	2	0.0023 min^{-1}	0.994	0.0221	0.939
		3	0.0025 min^{-1}	0.998	0.0236	0.926
		4	0.0022 min^{-1}	0.998	0.0223	0.919
Fe^{3+}	5:10:1	2	0.0017 min^{-1}	0.973	0.0158	0.983
		3	0.0019 min^{-1}	0.989	0.0171	0.945
		4	0.0017 min^{-1}	0.984	0.0223	0.985
	10:10:1	2	0.0018 min^{-1}	0.996	0.0212	0.920
		3	0.0022 min^{-1}	0.993	0.0242	0.953
		4	0.0019 min^{-1}	0.993	0.0282	0.934
	10:20:1	2	0.0020 min^{-1}	0.995	0.0240	0.930
		3	0.0024 min^{-1}	0.997	0.0261	0.939
		4	0.0021 min^{-1}	0.996	0.0288	0.916
Fe^{0}	5:10:1	2	0.0015 L/min mg	0.878	0.0182	0.863
		3	0.0014 L/min mg	0.916	0.0135	0.861
		4	0.0012 L/min mg	0.874	0.0183	0.902
	10:10:1	2	0.0019 L/min mg	0.880	0.0188	0.808
		3	0.0017 L/min mg	0.938	0.0157	0.868
		4	0.0016 L/min mg	0.919	0.0198	0.900
	10:20:1	2	0.0016 L/min mg	0.861	0.0205	0.936
		3	0.0014 L/min mg	0.878	0.0163	0.940
		4	0.0012 L/min mg	0.842	0.0200	0.920

Table 9
Degradation by-products generated from Fenton reactions using different iron types

Compound	Fe^{2+} and Fe^{3+}	Fe^0
TCE	Phosgene and dichloroacetyl chloride	Ethene, ethane, and vinyl chloride
2,4-DCP	Chlorohydroquinone, 2-chloro-1,4-benzoquinone, and 4,6-dichlororesorcinol	Hydroquinone and catechol
1,4-D	1,2-Ethanediol monoformate, 1,2-ethanediol diformate, formic acid, and methoxyacetic acid	1,2-Ethanediol monoformate, 1,2-ethanediol diformate, formic acid, and methoxyacetic acid
TCP	1,3-Dichloro-2-propanone and 2,3-dichloro-1-propene	Isopropanol and propionic aldehyde

The explanation for observing different by-products for Fe^0 is the same as the cases of TCE and 2,4-DCP.

4. Conclusions

This research attempted to compare the mineralization and biodegradability increase and their combination of TCE, 2,4-DCP, 1,4-D and TCP by Fenton reagents with three different types of iron, Fe^{2+}, Fe^{3+}, and Fe^0. Regardless of the iron type, most of the mineralization occurred within 120 min for TCE, 2,4-DCP, 1,4-D and 180 min for TCP while the biodegradability increased predominantly within 60 min for all four compounds. Fe^{2+} was more effective than Fe^{3+} and Fe^0 in the DOC reduction except for 2,4-DCP which Fe^0 provided slightly more mineralization than Fe^{2+}. For 1,4-D, the mineralization was very limited for all three iron types. The contaminant was partially degraded resulting in large amounts of biodegradability increase. The effect of iron type on biodegradability increase was not as obvious as that on mineralization; different types of iron generated comparable biodegradability increase fractions. The most effective iron type for biodegradability increase was not the same for all four compounds. The best types of iron for the combination of DOC elimination and biodegradability increase were controlled by the most effective types of iron for DOC elimination. Higher H_2O_2 doses increased the mineralization efficiency while faster mineralization and biodegradability increase kinetics based on the rate constant trends were observed at higher Fe amounts. pH within the range studied did not substantially affect the degradation efficiency. There was no trend between the degradation kinetics and pH; comparable rate constants were obtained at different pH values for most cases. Some of the degradation by-products identified were agreeable with previous studies while some have not been reported. For TCE, 2,4-DCP, and TCP, which are chlorinated compounds, the degradation by-products were different for Fe^0 catalyzed Fenton degradation due to the reductive effect (from Fe^0). For a future study, it is recommended that the by-products are quantified before and after BDOC incubation, and with reaction time to see which of them contribute to BDOC and to generate degradation pathways. In addition, finding or developing models that can better describe mineralization and BDOC increase kinetics should be attempted.

References

[1] L. Mater, E.V.C. Rosa, J. Berto, A.X.R. Correa, P.R. Schwingel, C.M. Radetski, A simple methodology to evaluate influence of H_2O_2 and Fe^{2+} concentrations on the mineralization and biodegradability of organic compounds in water and soil contaminated with crude petroleum, J. Hazard. Mater. 149 (2007) 379–386.
[2] A. Lopez, M. Pagano, A. Volpe, A.C. Di Pinto, Fenton's pre-treatment of mature landfill leachate, Chemosphere 54 (2004) 1005–1010.
[3] E.S. Batarseh, D.R. Reinhart, L. Daly, Liquid sodium ferrate and Fenton's reagent for treatment of mature landfill leachate, J. Environ. Eng. ASCE 133 (2007) 1042–1050.
[4] J. Bacardit, A. Hultgren, V. Garcia-Molina, S. Esplugas, Biodegradability enhancement of wastewater containing 4-chlorophenol by means of photo-Fenton, J. Adv. Oxid. Technol. 9 (2006) 27–34.
[5] O. Gonzalez, C. Sans, S. Esplugas, Sulfamethoxazole abatement by photo-Fenton, J. Hazard. Mater. 146 (2007) 459–464.
[6] M.J. Farre, X. Domenech, J. Peral, Combined photo-Fenton and biological treatment for diuron and linuron removal from water containing humic acid, J. Hazard. Mater. 147 (2007) 167–174.
[7] E. Khan, R.W. Babcock Jr., T.M. Hsu, H. Lin, Mineralization and biodegradability enhancement of low level *p*-nitrophenol in water using Fenton's reagent, J. Environ. Eng. ASCE 131 (2005) 327–331.
[8] P.M. Huck, Measurement of biodegradable organic matter and bacterial growth potential in drinking water, J. Am. Water Work Assoc. 82 (1990) 78–86.
[9] E. Khan, R.W. Babcock Jr., I.H. Suffet, M.K. Stenstrom, Method development for measuring biodegradable organic carbon in reclaimed and treated wastewaters, Water Environ. Res. 70 (1998) 1025–1035.
[10] J.J. Pignatello, Dark and photo assisted iron(3+)-catalyzed degradation of chlorophenoxy herbicides by hydrogen peroxide, Environ. Sci. Technol. 26 (1992) 944–951.
[11] W.Z. Tang, R.Z. Chen, Decolorization kinetics and mechanisms of commercial dyes by H_2O_2/iron powder system, Chemosphere 32 (1996) 947–958.
[12] R.J. Watts, A.P. Jones, P.-H. Chen, A. Kenny, Mineral-catalyzed Fenton-like oxidation of sorbed chlorobenzenes, Water Environ. Res. 66 (1997) 269–275.
[13] G. Chen, E.G. Hoag, P. Chedda, F. Nadim, B.A. Woody, G.M. Dobbs, The mechanism and applicability of in situ oxidation of trichloroethylene with Fenton's reagent, J. Hazard. Mater. B87 (2001) 171–186.
[14] K.R. Weeks, C.J. Bruell, N.R. Mohanty, Use of Fenton's reagent for the degradation of TCE in aqueous systems and soil slurries, Soil Sediment Contam. 9 (2000) 331–345.
[15] C.J. Yeh, H.M. Wu, T.C. Chen, Chemical oxidation of chlorinated non-aqueous phase liquid by hydrogen peroxide in natural sand systems, J. Hazard. Mater. 96 (2003) 29–51.
[16] F. Al Momani, Biodegradability enhancement of 2,4-dichlorophenol aqueous solution by photo-Fenton reaction, Environ. Eng. Sci. 23 (2006) 722–733.
[17] E. Chamarro, E. Marco, S. Esplugas, Use of Fenton reagent to improve organic chemical biodegradability, Water Res. 35 (2001) 1047–1051.
[18] W. Chu, C.Y. Kwan, K.H. Chan, S.K. Kam, A study of kinetic modelling and reaction pathway of 2,4-dichlorophenol transformation by photo-Fenton-like oxidation, J. Hazard. Mater. 121 (2005) 119–126.
[19] C.-C. Liu, D.-H. Tseng, C.-Y. Wang, Effects of ferrous ions on the reductive dechlorination of trichloroethylene by zero-valent iron, J. Hazard. Mater. 136 (2006) 706–713.
[20] H. Song, E.R. Carraway, Catalytic hydrodechlorination of chlorinated ethenes by nanoscale zero-valent iron, Appl. Catal. B: Environ. 78 (2008) 53–60.
[21] R. Cheng, J.-L. Wang, W.-X. Zhang, Comparison of reductive dechlorination of *p*-chlorophenol using Fe^0 and nanosized Fe^0, J. Hazard. Mater. 144 (2007) 334–339.
[22] I. Sanchez, F. Stuber, J. Font, A. Fortuny, A. Fabregat, C. Bengoa, Elimination of phenol and aromatic compounds by zero valent iron and EDTA at low temperature and atmospheric pressure, Chemosphere 68 (2007) 338–344.
[23] M.A. Beckett, I. Hua, Enhanced sonochemical decomposition of 1,4-dioxane by ferrous iron, Water Res. 37 (2003) 2372–2376.
[24] K.C. Namkung, A. Aris, P.N. Sharratt, Characterization of effects of selected organic substances on decomposition of hydrogen peroxide during Fenton reaction, Water Sci. Technol. 49 (2004) 129–134.
[25] C.-G. Kim, H.-J. Seo, B.-R. Lee, Decomposition of 1,4-dioxane by advanced oxidation and biochemical process, J. Environ. Sci. Health A 41 (2006) 599–611.
[26] F. Hunter, Fenton's treatment of 1,2,3-trichloropropane: chemical reaction byproducts, pathway, and kinetics, Chem. Oxid. 6 (1997) 50–71.
[27] W.Z. Tang, C.P. Huang, 2,4-Dichlorophenol oxidation kinetics by Fenton's reagent, Environ. Sci. Technol. 17 (1996) 1371–1378.
[28] B.G. Kwon, D.S. Lee, N. Kang, Characteristics of *p*-chlorophenol oxidation by Fenton's reagent, Water Res. 33 (1999) 2110–2118.
[29] M.C. Lu, J. Chen, C. Chang, Oxidation of dichlorvos with hydrogen peroxide using ferrous ion as catalyst, J. Hazard. Mater. 65 (1999) 277–288.
[30] A.L. Teel, C.R. Warberg, D.A. Atkinson, R.J. Watts, Comparison of mineral and soluble iron Fenton's catalysts for the treatment of trichloroethylene, Water Res. 35 (2001) 977–984.
[31] V. Maurino, P. Calza, C. Minero, E. Pelizzetti, M. Vincenti, Light-assisted 1,4-dioxane degradation, Chemosphere 35 (1997) 2675–2688.
[32] M.I. Stefan, J.R. Bolton, Mechanism of the degradation of 1,4-D in dilute aqueous solutions using the UV/hydrogen peroxide process, Environ. Sci. Technol. 32 (1998) 1588–1595.
[33] J.H. Suh, M. Mohseni, A study on the relationship between biodegradability enhancement and oxidation of 1,4-dioxane using ozone and hydrogen peroxide, Water Res. 38 (2004) 2596–2604.